Finite Size Effects in Antiferromagnetic NiO Nanoparticles

R. H. Kodama,[1,2] Salah A. Makhlouf,[2,3] and A. E. Berkowitz[1,2]
[1]*Physics Department, University of California at San Diego, La Jolla, California 92093*
[2]*Center for Magnetic Recording Research, University of California at San Diego, La Jolla, California 92093*
[3]*Physics Department, Assiut University, Assiut 71516, Egypt*
(Received 1 April 1997)

Antiferromagnetic NiO nanoparticles exhibit anomalous magnetic properties, such as large moments, and coercivities and loop shifts of up to 10 kOe. This behavior is difficult to understand in terms of 2-sublattice antiferromagnetic ordering which is accepted for bulk NiO. Numerical modeling of spin configurations in these nanoparticles yields 8-, 6-, or 4-sublattice configurations, indicating a new finite size effect, in which the reduced coordination of surface spins causes a fundamental change in the magnetic order throughout the particle. The relatively weak coupling between the sublattices allows a variety of reversal paths for the spins upon cycling the applied field, resulting in large coercivities and loop shifts. [S0031-9007(97)03838-6]

PACS numbers: 75.50.Tt, 75.10.Hk, 75.30.Pd, 75.50.Ee

Magnetism of small particles has generated increasing interest due to their unique magnetic properties as well as their technological applications [1]. Antiferromagnetic nanoparticles (AFN) have recently gained increased attention by virtue of their potential for exhibiting magnetization reversal by quantum tunneling [2,3]. In 1961 Néel suggested that fine particles of an antiferromagnetic material should exhibit magnetic properties such as superparamagnetism and weak ferromagnetism [4]. Néel attributed the permanent magnetic moment to an uncompensated number of spins on two sublattices. Indeed, large magnetic moments in AFN have been observed [5–7]; however, their origin is not clear. Some investigators attributed these moments to nonstoichiometry, presence of superparamagnetic metallic nickel clusters, or Ni^{3+} ions within the NiO lattice [8]. However, a recent report [9] has shown that these moments are only slightly changed by mild reduction (to eliminate Ni^{3+}) or oxidation (to eliminate Ni metal). Therefore, the superparamagnetism in NiO was attributed to incomplete compensation between AF sublattices.

In this Letter we report an experimental investigation of NiO nanoparticles with average size ranging from 50 to 800 Å. Remarkable properties include coercivities and loop shifts of up to 10 kOe, as well as moments much larger than predicted by a 2-sublattice model. We also present calculations of equilibrium spin configurations in NiO nanoparticles, based on literature values of exchange constants, which result in 8-, 6- or 4-sublattice spin ordering. This represents a new finite size effect, in which the reduced coordination of surface spins causes a fundamental change in the magnetic order throughout the particle. The multisublattice ordering allows for higher net moments, as well as a variety of reversal paths for the spins upon cycling the applied field, consistent with the observed simultaneous coercivity and loop shift.

NiO nanoparticles of various sizes were prepared by calcining portions of a dried gel of chemically precipitated $Ni(OH)_2$ in air for 3 h at various temperatures as described elsewhere [10]. X-ray diffraction patterns indicate single phase fcc NiO. The particle size was estimated from both x-ray diffraction line broadening using a modified Debye-Scherrer method [11], and BET surface area measurements assuming spherical particles. Preliminary TEM studies are consistent with these size determinations, and suggest platelet-shaped particles.

The permanent magnetic moment per particle was experimentally estimated as follows. The linear parts of the 5 K magnetization curves at high fields were extrapolated to zero field to estimate the intrinsic moment per gram. Using the average particle size and the density of bulk NiO, the moment per particle was estimated. We also performed calculations to determine the average moment for a 2-sublattice model. These consist of simply counting the spins on each sublattice, assuming the fcc Type-II antiferromagnetic order found in bulk NiO [12,13] (in contrast to the calculations detailed below which do not assume this type of order). We assumed $2\mu_B$ per Ni^{2+} ion [14], used a spherical shape, and varied the center position of the sphere within the unit cell in order to obtain a statistical average of 10^4 such particles. Over the size range 53 to 315 Å, the experimental moment was 5–10 times larger than the calculated moment. For example, we measure 700 μ_B per particle for the 150 Å sample, whereas the 2-sublattice model predicts 80 μ_B. Based on these considerations, the measured moment seems inconsistent with the 2-sublattice model.

Large coercivities and shifted hysteresis loops are observed for all samples after field cooling. Hysteresis loops measured at 5 K for the 315 Å diameter particles both zero field cooled (ZFC) and field cooled (FC) in 20 kOe from 340 K (above the superparamagnetic $T_B \approx$ 300 K, but below the bulk $T_N = 523$ K) are shown in Fig. 1. The ZFC coercivity is 10 kOe, the moment is unsaturated, and the loop is open up to 70 kOe. The FC loop is slightly broadened and has a loop shift of 10 kOe.

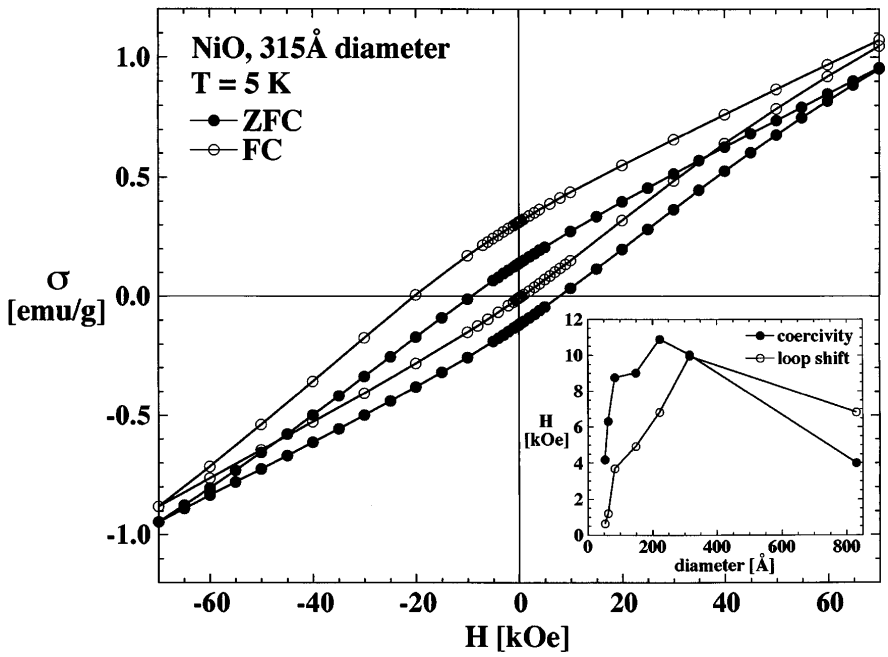

FIG. 1. Hysteresis loops at 5 K of 315 Å NiO particles; ZFC and FC from 340 K in 20 kOe. Inset shows the coercivity and loop shift as functions of particle size.

The coercivity and loop shift versus particle diameter are shown in the inset of Fig. 1. Very large coercivities and loop shifts (>10 kOe) are obtained for the intermediate-sized particles with 220 Å $\leq d \leq$ 315 Å.

The hysteresis of a collection of 2-sublattice AFN, having net moments due to uncompensated spins, can be described in terms of a Stoner-Wohlfarth type model [15], in which the spin axis has two or more metastable orientations which depend on the magnetic anisotropy and the applied field. Within this model, *major* hysteresis loops are symmetric since the magnetocrystalline anisotropy has inversion symmetry. If, however, the field is not sufficient to reverse the particle moment (i.e., minor hysteresis loop), one could obtain a shifted loop with no hysteresis. Therefore, a simultaneous loop shift and coercivity can only be described in terms of this model if one attributes it to a broad distribution of reversal fields, both greater and less than the maximum applied field. In order to better understand the magnetic behavior of AFN, we have employed calculations of equilibrium spin configurations similar to those developed in recent studies of $NiFe_2O_4$ nanoparticles [16]. The basic features of the model are (1) exchange and anisotropy constants obtained from an inelastic neutron scattering study by Hutchings and Samuelsen [14]; (2) classical spins in a NaCl structure; (3) a fraction of broken exchange bonds between surface spins, with exchange bonds between surface and core spins unchanged; (4) uniaxial anisotropy applied to surface spins with an axis corresponding to the dipole moment of the neighboring anion positions (approximately radial); (5) dynamic scaling of the nearest neighbor exchange splitting via the theory of exchange striction [17]; and (6) finite temperatures simulated by applying random perturbations to the spin orientations between relaxation steps. Hutchings and Samuelsen used an orthorhombic form for the anisotropy:

$$E_A = D_1 S_z^2 + D_2 S_y^2 , \tag{1}$$

where x is the easy axis $\langle 11\bar{2} \rangle$ and z is the hard axis $\langle 111 \rangle$. The structure of NiO is actually rhombohedral so for the calculations we instead used a sixfold symmetric form, as observed via torque measurements [18]. The total spin Hamiltonian used was

$$\mathcal{H} = \sum_i^{\{\text{all spins}\}} \left[g_i \mu_B \mathbf{S}_i \cdot \left(-\vec{\mathbf{H}} + \frac{1}{2} \sum_j^{\text{n.n}} \frac{2 J_{ij} S_j}{g_i \mu_B} \hat{\mathbf{S}}_j \right) + D_1 \hat{S}_{zi}^2 - (D_2/18) \cos 6\phi_i \sin^6 \theta_i \right],$$

where θ_i and ϕ_i are the conventional spherical coordinates corresponding to the direction of the ionic spin $\hat{\mathbf{S}}_i$ with ϕ_i referenced to the $\langle 11\bar{2} \rangle$ direction. The factor of 18 results from matching the leading terms in a small-ϕ expansion of our Hamiltonian to that of Eq. (1). The exchange and anisotropy parameters used are the following (in units of K) [14]:

$$J_1^+ = -15.7, \qquad J_1^- = -16.1, \qquad J_2 = 221 ,$$
$$D_1 = 1.13, \qquad D_2 = 0.06 ,$$

where exchange constants are J_1^- between nearest neighbors in the same (111) plane (normally ferromagnetically aligned), J_1^+ between nearest neighbors in adjacent (111) planes (normally antiferromagnetically aligned), and J_2 between next nearest neighbors. The difference between J_1^+ and J_1^-, associated with the rhombohedral contraction

occuring below the Néel point, is predicted by the theory of exchange striction [17] to vary as

$$(J_1^+ - J_1^-) = 2j\overline{S}^2, \quad (2)$$

where $\overline{S}$ is the average spin and $j = 0.26$ K [14]. $\overline{S}$ can be described as an order parameter for the 2-sublattice state. Since we find substantial deviations from the 2-sublattice state, we calculate $\overline{S}$ [19] after each step of the relaxation procedure and rescale J_1 according to Eq. (2). The magnitude of the uniaxial surface anisotropy was chosen to be 2 K, which is a reasonable value based on EPR determinations of the magnetocrystalline anisotropy of Ni^{2+} ions in bulk oxide crystals with sites of low symmetry [20].

Calculations on spherical particles of different diameters were performed in order to determine the onset of the multisublattice spin state. Figure 2 shows the average order parameter $\overline{S}$ and number of sublattices (differing in spin direction by $> 3°$) for 30 different particles in zero applied field as a function of particle diameter. Two curves are plotted for relatively smooth particles with different values of the "broken bond density" (BBD), and a third curve is plotted for a rougher particle. Roughness is created by removing surface cations at random and taking off any asperities afterward, as described in Ref. [16]. The results indicate that the order parameter approaches unity as the particle size increases, while the average number of sublattices is close to 8 for smaller sizes and approaches 2 as the size increases. The size threshold for this behavior is strongly dependent on parameters of the surface. Multisublattice configurations result in average moments 4 times larger than the 2-sublattice calculations mentioned above, for BBD = 0.8 and 4 Å rms roughness (calculated for particles 25–50 Å).

Hysteresis loops were calculated for both spherical and platelet shaped particles, and in both cases we found large coercivities and loop shifts. A simulated field cooling procedure was done, in which perturbations of 400 K/spin were applied and the spin configuration was allowed to relax in the presence of a 100 kOe field. The perturbation was applied several times, followed by relaxation of the spin configuration each time, to find the lowest energy state. Field cooling with smaller perturbations or smaller fields causes the sign of the loop shift to depend on the initial spin configuration. An example of such a calculation is shown in Fig. 3, where a 44 Å diameter, 17 Å thick platelet is used, with the field applied in the plane of the platelet, which has ⟨111⟩ orientation. The broken bond density in this case was 0.5. The curve is qualitatively similar to those obtained experimentally. Since the magnetic properties are complex functions of the particles' net moments, sizes, morphologies, and crystal orientations, a more quantitative comparision with experiment will require addressing the formidable task of modeling distributions of these properties. Figure 4 shows the corresponding spin configurations in the positive and negative remanent states, which illustrates the multisublattice state and shows that the two states are qualitatively different, not simply 180° rotations from each other. It is evident that the intersublattice angles are not fixed, but can change substantially upon cycling the field, giving rise to a variety of reversal paths for the spins. We find that surface anisotropy and multisublattice states are key ingredients to produce simultaneous coercivities and shifted loops.

Based on our calculated spin configurations, we find that the stability of the 2-sublattice state (versus multisublattice states) in *bulk* NiO is directly related to the $J_1^+ - J_1^-$ splitting. Since the rhombohedral contraction

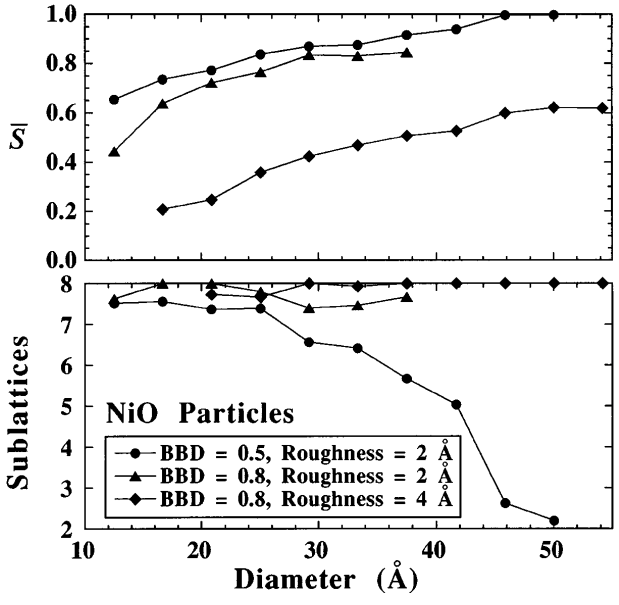

FIG. 2. Calculated average order parameter $\overline{S}$ and average number of sublattices for 30 different NiO particles in zero applied field as a function of diameter. The surface broken bond density (BBD) and rms roughness amplitude are indicated in the legend.

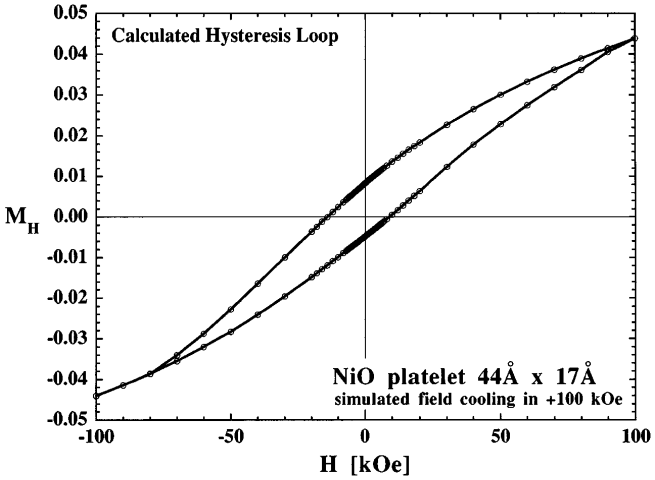

FIG. 3. Calculated "field cooled" hysteresis loop for a 44 Å diameter, 17 Å thick NiO platelet. Field is applied in the plane of the platelet, which has ⟨111⟩ orientations.

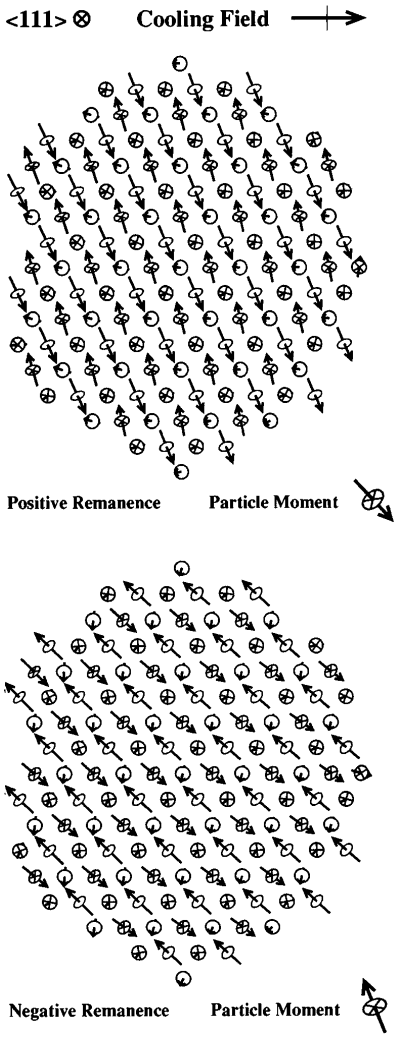

FIG. 4. Calculated spin configurations for the same platelet as in Fig. 3, in the positive and negative remanent states (i.e., zero field). The central cross section of the particle is shown. The disks attached to the spin vectors indicate their orientation in 3D; those decorated with a $\times$ are pointing into the page.

is known to diminish with increasing temperature [17], multisublattice states should become more prevalent at higher temperatures. We suggest that considerations of multisublattice ordering may be useful in describing critical behavior, even in bulk NiO.

In summary, we have observed moments in AFN which are too large to be explained by a 2-sublattice model, and large coercivities and loop shifts at low temperatures. These observations are consistent with multisublattice spin configurations which follow directly from bulk exchange parameters and considerations of low coordination at surface sites. We show that this finite size effect can have a profound effect on low temperature hysteresis properties, giving rise to simultaneous coercivity and loop shift when surface and bulk anisotropies are included. We suggest that multisublattice states become more important at high temperatures, even in bulk materials.

This work was supported in part by the MRSEC Program of the NSF under Award No. DMR-9400439. The support of S. A. M. by the Fullbright commission is gratefully acknowledged. The helpful advice of F. E. Spada in sample preparation is acknowledged. TEM investigations by G. A. Fischer and M. L. Rudee are acknowledged and will be reported elsewhere.

[1] R. W. Chantrell and K. O'Grady, *Applied Magnetism*, edited by R. Gerber et al. (Kluwer Academic Publishers, The Netherlands, 1994), p. 113.
[2] M. M. Ibrahim, S. Darwish and M. Seehra, Phys. Rev. B **51**, 2955 (1995).
[3] S. Gider, D. Awschalom, T. Douglas, S. Mann, and M. Chaparala, Science **268**, 77 (1995).
[4] L. Neel, in *Low Temp. Phys.*, edited by C. Dewitt, B. Dreyfus, and P. D. de Gennes (Gordon and Beach, New York, 1962), p. 413.
[5] J. T. Richardson and W. O. Milligan, Phys. Rev. **102**, 1289 (1956).
[6] J. Cohen, K. M. Creer, R. Pauthenet, and K. Srivastava, J. Phys. Soc. Jpn. **17**, Suppl. B-I, 685 (1962).
[7] W. J. Schuele and V. D. Deetscreek, J. Appl. Phys. **33**, 1136 (1962).
[8] I. S. Jacobs and C. P. Bean, in *Magnetism*, edited by G. T. Rado and H. Suhl (Academic Press, New York, 1963), Vol. III, p. 294.
[9] J. T. Richardson, D. I. Yiagas, B. Turk, K. Forster, and M. V. Twigg, J. Appl. Phys. **70**, 6977 (1991).
[10] Salah A. Makhlouf, F. T. Parker, F. E. Spada, and A. E. Berkowitz, J. Appl. Phys. **81**, 5561 (1997).
[11] G. K. Williamson and W. H. Hall, Acta Metall. **1**, 22 (1953).
[12] P. W. Anderson, Phys. Rev. **79**, 705 (1950).
[13] W. L. Roth, Phys. Rev. **110**, 1333 (1958).
[14] M. T. Hutchings and E. J. Samuelsen, Phys. Rev. B **6**, 3447 (1972).
[15] E. C. Stoner and E. P. Wohlfarth, Philos. Trans. Roy. Soc. London **A240**, 599 (1948).
[16] R. H. Kodama, A. E. Berkowitz, E. J. McNiff, Jr., and S. Foner, Phys. Rev. Lett. **77**, 394 (1996); J. Appl. Phys. **81**, 5552 (1997).
[17] M. E. Lines and E. D. Jones, Phys. Rev. **139**, A1313 (1965); L. C. Bartel and B. Morosin, Phys. Rev. B **3**, 1039 (1971).
[18] K. Kurosawa, M. Miura, and S. Saito, J. Phys. C: Solid State Phys. **13**, 1521 (1980).
[19] We compute $\overline{S}$ for any given spin configuration as
$$\overline{S} = \max_{j=1,2,3,4} \left| \frac{1}{N} \sum_{i=1}^{N} (-1)^{k_{ij}} \mathbf{S}_i \right|,$$
where N is the number of spins, and k_{ij} is defined as $k_{i1} = \mathbf{P}_i \cdot (1,1,1)/a$, $k_{i2} = \mathbf{P}_i \cdot (1,1,-1)/a$, $k_{i3} = \mathbf{P}_i \cdot (1,-1,1)/a$, and $k_{i4} = \mathbf{P}_i \cdot (-1,1,1)/a$, where $\mathbf{P}_i$ is the position of the ith spin and a is the cubic lattice parameter. We essentially calculate the order parameter for each possible (111) type ordering plane, and take the largest value.
[20] A. K. Petrosyan and A. A. Mirzakhanyan, Phys. Status Solidi B, **133**, 315 (1986).